HIGHLIGHTS

- Peach flesh metabolome is strongly influenced by UV-B exposure;
- Phenolics, terpenoids and phytoalexins highly responded to UV-B;
- Decreased levels of most metabolic classes were detected after 24 h;
- Accumulation of most metabolic classes was observed after 36 h;
- UV-B radiation does not penetrate peach skin

The outer influences the inner: postharvest UV-B radiation modulates peach flesh metabolome although shielded by the skin

Marco SANTIN [1*], Annamaria RANIERI [1,2], Marie-Theres HAUSER [3], Begoña MIRAS-MORENO [4,6], Gabriele ROCCHETTI [4], Luigi LUCINI [4], Åke STRID [5], Antonella CASTAGNA [1,2]

[1] Department of Agriculture, Food and Environment, University of Pisa, via del Borghetto 80, 56124 Pisa, Italy

[2] Interdepartmental Research Center Nutrafood ''Nutraceuticals and Food for Health'', University of Pisa, Via del Borghetto 80, 56124 Pisa, Italy

[3] Department of Applied Genetics and Cell Biology, University of Natural Resources and Life Sciences, Muthgasse 18, 1190 Vienna, Austria

[4] Department for Sustainable Food Process, Università Cattolica del Sacro Cuore, Via Emilia Parmense, 84, 29122 Piacenza, Italy

[5] School of Science and Technology and Örebro Life Science Center, Örebro University, Örebro, Sweden

[6] Council for Agricultural Research and Economics- Research Centre for Genomics and Bioinformatics (CREA-GB), via San Protaso 302, 29017, Fiorenzuola d'Arda, PC, Italy

Marco Santin: marco.santin@agr.unipi.it
Annamaria Ranieri: anna.maria.ranieri@unipi.it
Marie-Theres Hauser: marie-theres.hauser@boku.ac.at
Begoña Miras-Moreno: mariabegona.mirasmoreno@unicatt.it
Gabriele Rocchetti: gabriele.rocchetti@unicatt.it
Luigi Lucini: luigi.lucini@unicatt.it
Åke Strid: ake.strid@oru.se
Antonella Castagna: antonella.castagna@unipi.it

Corresponding author
Marco Santin
Department of Agriculture, Food and Environment, University of Pisa, via del Borghetto 80, 56124 Pisa, Italy
Email address: marco.santin@agr.unipi.it

ABSTRACT

UV-B-driven modulation of secondary metabolism in peach fruit by enhancing the biosynthesis of specific phenolic subclasses, is attracting interest among consumers. However, current literature explored the UV-B-induced metabolic changes only in peach skin subjected to direct UV-B irradiation. Accordingly, this study aimed to understand whether UV-B radiation penetrates the fruit skin and is able to induce metabolic changes also within the inner flesh. Peaches were UV-B-irradiated either 10 or 60 min, and the flesh was sampled after 24 and 36 h. Non-targeted metabolomics revealed that UV-B has a strong impact on peach flesh metabolome, determining an initial decrease after 24 h, followed by an overall increase after 36 h, particularly for terpenoids, phenylpropanoids, phytoalexins and fatty acids in the 60 min UV-B-treated samples (+150.02, +99.14, +43.79 and +25.44 log_2FC, respectively). Transmittance analysis indicated that UV-B radiation does not penetrate below the skin, suggesting a possible signalling pathway between tissues.

KEYWORDS

UV-B radiation; phenolics; peach fruit; *Prunus persica*; metabolomics

1. INTRODUCTION

In the last decades, consumers have grown awareness about overall food quality, therefore the demand of fruit and vegetables rich in health-promoting compounds has progressively increased. Peach (*Prunus persica* L.) is a worldwide consumed stone fruit, which plays a key role in the Mediterranean diet. Its ever-increasing popularity arises due not only to its particularly appreciated sensory attributes, but also to its high content of nutraceutical compounds. Among them, peach fruit is particularly rich in phenolics, carotenoids and ascorbic acids, which are strong antioxidants within plant phytochemicals. Phenolic compounds represent a complex and diversified class of plant secondary metabolites, which fulfil many fundamental functions during plant lifespan e.g. as antibacterials, antivirals, antifungals, deterrents for herbivores, attractors for pollinators and seed dispersers, antioxidants, protectors against potentially harmful solar ultraviolet (UV) radiations and mechanical support for the plant itself (Cheynier, Comte, Davies, Lattanzio & Martens, 2013). Bioavailability of phenolics strictly depends on their chemical structure (e.g. molecular weight, glycosylation and/or esterification state, linked functional groups) the food matrix and the food processing operations performed before consumption (Acosta-Estrada, Gutiérrez-Uribe & Serna-Saldivar, 2014; Valdés, Cuervo, Salazar, Ruas-Madiedo, Gueimonde & Gonzàles, 2015). Once absorbed in the intestinal tract, the phenolic compounds enter the cardiovascular system where they can provide benefits for human health. In fact, many studies have observed a correlation between consumption of phenolics, especially flavonoids, and the reduction of the incidence of several diseases such as cancer, diabetes, asthma, hypertension, cardiovascular diseases, aged-related diseases and neurodegenerative disorders (e.g. Parkinson's and Alzheimer's diseases) (Shahidi & Ambigaipalan, 2015). The bioactive role of phenolic compounds, both in plants and human metabolism, is mainly due to their high scavenging activity towards reactive oxygen species (ROS), physiologically generated within the cells during the respiration process. However, their concentration within the plant or fruit can rapidly increase or decrease both in pre- and postharvest in response to many abiotic and biotic stressors, e.g. high/low temperature (Dreyer & Dietz, 2018),

drought/salinity conditions (Gupta, Palma & Corpas, 2015), attacks of pathogens (Camejo, Guzmán-Cedeño & Moreno, 2016) and high-energy UV-B radiations induced ROS (Hideg, Jansen & Strid, 2013), causing potential damages to many cellular components and macromolecules (Choudhury, Rivero, Blumwald & Mittler, 2017). Besides phenolics, peach fruit is rich in other health-promoting phytochemicals, e.g. carotenoids. Carotenoids are one of the most representative subclasses of the terpenoids class, mainly responsible for red, orange and yellow pigmentations of many organisms, (e.g. plants, bacteria, fungi, animals) (Rodriguez-Concepcion et al., 2018). Within the plant kingdom, they act as attractors for pollinators and seed dispersers, and protect the photosynthetic apparatus from ROS. Fundamental roles of carotenoids have been elucidated also in human metabolism. Indeed, their benefits for human health are mainly due to their antioxidant properties, and studies have correlated the consumption of several carotenoids with a reduced risk of cardiovascular diseases, low-density lipoprotein peroxidation and prostate cancer (Eggersdorfer & Wyss, 2018), with a key role also in bone homeostasis (Yamaguchi & Uchiyama, 2003) and eye health (Feeney et al., 2013) as precursors of vitamin A and retinoids (Kopsell & Kopsell, 2006).

UV-B radiation is a small fraction (280-315 nm) of the solar spectrum and represents the highest-energetic radiation reaching the earth's surface. UV-B is mainly absorbed by the stratospheric ozone layer, thus only 5% reaches the ground, depending on time, season, weather conditions and latitude (Nunez, Forgan & Roy, 1994). Contrarily to the past, when UV-B radiation was only considered a stressor for plant organisms (Jansen, Gaba & Grinnberg, 1998), it has been a few years since researchers identified an UV-B-activated signalling pathway mediated by the UV-B photoreceptor UV RESISTANCE LOCUS 8 (UVR8) (Rizzini et al., 2011). Such UV-B-specific pathway controls the upregulation of several phenylpropanoid genes, consequently increasing the production of phenolic compounds (Catola et al., 2017; Jansen, Hectors, O'Brien, Guisez & Potters, 2008; Santin, Lucini, Castagna, Rocchetti, Hauser & Ranieri, 2019b; Scattino et al., 2014) allowing the acclimation of plants to higher UV-B conditions and preventing damages caused by the UV-B-induced ROS. In the light of the positive correlation between UV-B radiation and phenolics content,

researchers have deeply investigated the UV-B-induced increase of phenolic compounds in fruit and vegetables, such as tomato (Castagna, Dall'Asta, Chiavaro, Galaverna & Ranieri, 2014), peach (Santin, Lucini, Castagna, Chiodelli, Hauser & Ranieri, 2018a; Santin et al, 2019b; Scattino et al., 2014), lettuce (Lee, Son & Oh, 2014), apple (Assumpção et al., 2018; Kokalj, Bizjak, Zlatić, Cigić, Hribar & Vidrih, 2016) and table grape (Sheng, Zheng, Shui, Yan, Liu & Zheng, 2018). Apart from the positive effect of the increased nutraceutical value, also shelf-life is boosted (Santin et al., 2019a). However, almost the entire relevant literature has investigated the UV-B-driven changes of phenolics only in the fruit skin, since it represents the outermost tissue and is therefore directly exposed to the UV-B radiation. It is also important to point out that most consumers use to peel the fruit before eating in order to remove the possible presence of harmful chemicals, e.g. pesticides and fungicides. Therefore, eliminating the beneficial enriched phenolics in the skin. In the light of above, and considering the scarcity of current literature about an "-omics" approach to investigate the UV-B effects on secondary metabolism, this work aimed to figure out whether UV-B exposure on peach fruit might influence the secondary metabolism also in the peach flesh and which metabolic classes are mainly responsive.

2. MATERIAL AND METHODS

2.1 Plant material and UV-B treatment

Organic peach fruit (*Prunus persica* L., cv Fairtime) were accurately selected to be homogeneous in colour, shape and dimension (8.1 cm average diameter), and eventual damaged or infected fruit were discarded. Several quality traits, e.g. titratable acidity, firmness and soluble solid content, were evaluated just before the UV-B treatments and in correspondence of the recovery timepoints, and results are reported in Santin et al. (2019a). Peaches used for this study showed a firmness value of 25.60 N as soon as they were purchased from the supermarket, which defined the stage of the fruit as "ready to buy" according to Valero, Crisosto and Slaughter (2007). After the UV-B treatment and during the recovery time, peaches underwent a physiological decrease of firmness due to the

ripening process, displaying a firmness value of < 18 N, thus reaching the "ready to eat" stage (Valero, Crisosto and Slaughter, 2007).

Once arrived at the laboratory, five peaches were immediately sampled and therefore represented time point 0 (T_0). Remaining peaches were divided into controls and either 10 min or 60 min UV-B-treated ones. The climate chambers used for the UV-B irradiation were set to room temperature (24 °C) and equipped with four UV-B tubes (Philips Ultraviolet-B Narrowband, TL 20W/01 – RS, Koninklijke Philips Electronics, Eindhoven, The Netherlands; emission spectrum reported in Fig. S1) and white light tubes. At fruit height, peaches were given a total irradiance of 6.42 kJ m^{-2} (1.39 kJ m^{-2} UV-B + 5.03 kJ m^{-2} white light) and 38.53 kJ m^{-2} (8.33 kJ m^{-2} UV-B + 30.20 kJ m^{-2} white light) in the 10 min and 60 min treatment, respectively. Control peaches were exposed to just white light. Peach flesh (1.5 cm thick just below the skin) from the UV-B exposed side of each fruit was sampled with scalpels and tweezers after 24 h and 36 h from the end of the UV-B exposure. A schematic representation of the experimental setup has been reported as Fig. S2. During such recovery period, peaches were kept at room temperature (24 °C) to simulate a typical domestic storage. Samples were dipped into liquid nitrogen, freeze-dried and stored at -80 °C until further analyses. Five peaches per treatment (control, UV-B 10 min and UV-B 60 min) were sampled for each recovery time, and the flesh from each fruit was kept and analysed separately.

2.2 Extraction and untargeted metabolomics profiling

Samples were extracted and analysed as described by Santin et al. (2018a). Briefly, 1g of sample was homogenized in 10 mL of 80% methanol solution (v/v) acidified with 0.1% formic acid through a homogenizer-assisted extraction (Ultra-turrax; Ika T25, Staufen, Germany). The extracts were centrifuged at 6000 g for 10 min at 4 °C, filtered using 0.22 µm cellulose syringe filters and stored at −18 °C until analysis. Metabolites were then screened in the range 100–1200 m/z using an ultra-high-performance liquid chromatography (UHPLC) coupled to a quadrupole-time-of-flight high-resolution mass spectrometer via an electrospray ionization system (UHPLC-ESI-QTOF-MS)

in positive FULL SCAN mode. The analytical conditions used for both chromatography and mass spectrometry are detailed in previous works from our research group (Santin et al., 2019b).

The raw mass features from metabolomic profiling were analyzed using the Agilent Profinder B.06 software (Agilent technologies, Santa Clara, CA, USA) and considering the 'find-by-formula' algorithm. The high confidence in identification was recursively reached by coupling accurate mass together with isotope pattern (isotopic spacing and ratio), adopting a 5-ppm tolerance for mass accuracy. In particular, compounds were annotated by exploiting a custom database built combining Phenol Explorer (Phenol-Explorer 3.6; phenol-explorer.eu/) and PlantCyc 9.6 (Plant Metabolic Network, http://www.plantcyc.org) dataset.

Thereafter, polyphenols identified were also quantified according to their corresponding phenolic subclasses. In particular, methanolic standard solutions of single phenolics were injected into UHPLC/QTOF to achieve this goal. Cyanidin (2-(3,4-Dihydroxyphenyl) chromenylium-3,5,7-triol; anthocyanins), (+)-catechin (flavanols), luteolin (3′,4′,5,7-Tetrahydroxyflavone; flavones and other remaining flavonoids), resveratrol (3,4′,5-Trihydroxy-trans-stilbene; stilbenes), 5-pentadecylresorcinol (alkylphenols), tyrosol (tyrosols and other remaining low molecular weight phenolics), ferulic acid (trans-ferulic acid; hydroxycinnamics acids and other phenolic acids), sesamin (furofuran lignans) and matairesinol (dibenzylbutyrolactone and dihydroxydibenzylbutane lignans) were considered as representative of their respective phenolic class. All standard compounds were purchased from Extrasynthese (Genay, France) each having a purity > 98%. Calibration curves were built using a linear fitting (un-weighted and not forced to axis-origin) in the range 0.05–500 mg L^{-1}; a coefficient of determination $R^2 > 0.98$ was used as acceptability threshold for calibration purposes.

Finally, the software Mass Profiler Professional 12.6 (Agilent Technologies) was used to elaborate metabolomics-based data. In this regard, compound abundance was log2 transformed and normalized at the 75th percentile, following by a baselining procedure against the median of each compound in the metabolomic dataset. Multivariate statistics was then performed by using both

unsupervised and supervised approaches. In this regard, the unsupervised hierarchical cluster analysis (Euclidean distance, Ward's linkage) was performed to investigate the relatedness across the different treatments, whilst the orthogonal projection to latent structures discriminant analysis (OPLS-DA) was used as supervised modelling. In particular, the goodness-of-fit (R^2Y) and the goodness-of-prediction (Q^2Y) parameters have been inspected before conducting the variables importance in projection (VIP) approach. This latter was used to identify the best marker of the phenolic profiles observed, i.e. those compounds possessing a VIP score > 1 (i.e. the most discriminant compounds). A volcano plot analysis was also performed combining ANOVA ($p < 0.05$; Bonferroni multiple testing correction) and fold-change analysis (cut-off ≥ 2), then exporting the differential compounds to the PlantCyc pathway Tools software (Karp et al., 2010) for further elaborations. The resulting figures throughout the manuscript has been created by reporting the $\log_2$ fold-change values between the UV-B exposed peaches and the controls for each recovery time points, in order to better separate the effects of the UV-B treatments from the ones due to the physiological ripening process of the fruit.

2.3 Transmittance analysis across peach skin

Some peaches from the same batch (*Prunus persica* L., cv. Fairtime, "ready to buy" stage) were used for skin transmittance of light between 250 and 800 nm using spectrophotometry (Shimadzu UV1800 UV/VIS spectrophotometer in scanning transmission mode) and spectroradiometry (Optronics Laboratories OL756) with essentially the same results. Rectangular (35 by 15 mm) or circular (diameter 35 mm) patches of skin were removed from ripe fruit, whereafter all flesh was removed from the skin patch before measurements. As a comparison with the transmittance of yellow skin, particolored red *Prunus persica* (unknown cultivar obtained from a local supermarket) was also used for transmittance studies.

3. RESULTS AND DISCUSSION

3.1 Flesh is the main source of phenolic compounds in peach fruit

Phenolic compounds are involved in many essential processes and responses during plant development, e.g. reproduction, acclimation, resistance towards biotic and abiotic stresses. For this reason, when it comes to fruit, such phytochemicals are mostly concentrated in the skin since it represents the outermost tissue and consequently the first defence line against possible environmental stresses. With UHPLC-ESI-QTOF-MS, the concentration of phenolic subclass within both peach skin and flesh was measured and graphically presented in Fig. 1, while the full dataset is reported in Table S1. As expected, the profile of the phenolic composition was very complex within peach fruit, displaying a huge diversity of phenolic subclasses. More in detail, 27 phenolic subclasses were identified, comprising more than 400 phenolic compounds. Particularly, the most representative phenolic classes were flavonols, tyrosols, hydroxycinnamic acids and anthocyanins. On a fresh weight basis (Fig. 1A), the concentration of phenolics was 65% higher in the skin compared to the flesh. However, while concentration of flavonols, tyrosols and anthocyanins was higher in peach skin (+350%, +176% and +55%, respectively), hydroxycinnamic acids were more abundant in the flesh (+97%). Higher content of such phytochemicals in the skin of fruit has been already reported in previous analyses for peach (Saidani, Giménez, Aubert, Chalot, Betrán, & Gogorcena, 2017), mango (Agatonovic-Kustrin, Kustrin & Morton, 2018), apple (Lee, Chan & Mitchell, 2017) and grape (Gomes et al., 2019) and exhibited a cultivar dependency.

Nevertheless, considering the average pulp/skin weight ratio (25.5), and pit weight (8 g) of an individual Fairtime peach fruit, the contribution of the flesh weight is over 25 times compared to the skin (Fig. 1B). Consequently, 94% of phenolics derives from the flesh of a single peach, although their concentration in mg/kg is lower compared to the skin. Taking this into account, it is likely that also the content of other metabolic classes is higher in the flesh of an individual peach. This

confirms the importance to investigate whether and how UV-B radiation might affect metabolomic profiles also in the peach flesh.

3.2 An untargeted approach reveals that UV-B irradiation plays a key role in promoting metabolomics changes in the flesh of peaches

A metabolomic approach was used to understand whether the UV-B radiation was effective in inducing changes in the content of several secondary metabolism in the flesh of peaches. Coupling an untargeted UHPLC/QTOF-MS analysis with a comprehensive database for compounds identification from both primary and secondary metabolisms (PlantCyc), it was possible to detect more than 3000 metabolites. The complete dataset of the identified compounds is provided in Table S2.

A fold-change-based hierarchical clustering was performed (Fig. 2). The output of this unsupervised analysis revealed a first marked clustering between the controls and the UV-B-treated samples, regardless of the UV-B dose. This result clearly indicates an effect of UV-B irradiation in modulating the metabolomic profile in the peach flesh. Furthermore, the recovery time, 0 h, 24 h or 36 h, played also a role in influential a specific metabolite pattern. Indeed, sub-clusters originated among the control groups, which mainly reflect the recovery time. The short distance between the main clustering (separating the controls and the UV-B-treated samples) and the first sub-clustering (separating the groups according to the recovery time) suggested that the physiological ripening of the fruit is also a crucial factor in determining a specific metabolomic profile. The only outlier was the unirradiated group after 36 h, which clustered separately from the other control groups and among the UV-B-exposed groups after 24 h. Thereafter, we used OPLS-DA supervised modelling in order to check the impact of both UV-B radiation and recovery times when considering the database on polyphenols (Table S1). In this regard, the only OPLS-DA model showing an acceptable goodness-of-prediction (i.e. $Q^2 = 0.594$) was that built considering the recovery time (i.e. 24 *vs* 36 h) as main factors driving samples separation. The output of the OPLS-DA score plot is

reported in supplementary material together with the VIP discriminant markers allowing sample separation. This model clearly confirmed the impact of UV-B radiations and recovery times on the phenolic profiles observed, with lower differences in the UV-B-exposed groups after 36 h. In this regard, among the VIP discriminant markers (Table S1), we found 150 phenolic compounds, with a clear abundance of flavonoids (i.e. anthocyanins, flavones and flavonols), phenolic acids (mainly hydroxycinnamics) and lower-molecular-weight compounds (i.e. tyrosol derivatives).

Although no previous research has investigated the UV-B-induced metabolomic effect specifically on peach flesh, the metabolomic profile of peach skin was highly responsive to both UV-B radiation and recovery times. Specifically, Santin et al. (2018a) observed a strong rearrangement of the skin metabolome following either 10 min or 60 min of UV-B irradiation, which involved several metabolic classes, especially phenolics, terpenoids and lipids.

3.3 Secondary metabolites in peach flesh are differentially influenced by UV-B radiation and recovery time

Once elucidated that UV-B radiation influenced the metabolomic profile in the flesh of peaches, our aim was to investigate deeper which metabolic classes were mainly affected by the UV-B treatments, and whether such changes might influence the fruit quality. A Volcano analysis (FC threshold ≥ 2; p-value ≤ 0.05) was performed, and the resulting compounds were grouped to their respective metabolic classes. This way, it was possible to get a metabolic overview of the UV-B-induced response in the peach flesh. Results of the Volcano analysis for each metabolic class are graphically presented in Fig. 3, while the full list of the compounds resulting from the same analysis, together with the respective fold-change values and p-values, are reported in Table S3. In Fig. 3, as well as in the following Fig. 4 and 5, data are expressed as $\log_2$ fold-change between the UV-B-treated groups and the control group considering each recovery time point separately, in order to show the metabolic variations due only to the UV-B treatments and not to the normal process of ripening of the fruit.

Both 10 min and 60 min UV-B treatment determined a general decrease of secondary metabolites after 24 h with a particularly marked effect for terpenoids, phytoalexins and phenylpropanoid derivatives (-45, -18 and -5 log_2FC for 10 min, and -34, -27 and -16 log_2FC for 60 min UV-B, respectively, Fig. 3A). Such a decrease was slightly higher in the 60 min UV-B-treated samples for phenylpropanoids and phytoalexins, while the lower UV-B dose of 10 min was more effective than 60 min UV-B in decreasing the concentration of terpenoids. However, 36 h after the UV-B treatments (Fig. 3B), the pool of secondary metabolites underwent a general increase, and most UV-B-affected metabolic classes were the same mentioned before, i.e. terpenoids, phenylpropanoid derivatives and phytoalexins (+44.60, +25.43 and +12.12 log_2FC for 10 min, and +150.02, +99.14 and +43.79 log_2FC for 60 min UV-B, respectively). Moreover, an overall increase was also detected in the content of fatty acid derivatives (+19.80 log_2FC for 10 min and +25.44 log_2FC for 60 min UV-B, respectively), which were not affected in the 24 h recovery samples. The highest increase was observed for terpenoids, followed by phenolics, phytoalexins and fatty acid derivatives, showing an UV-B-dose dependent response for all the metabolic classes analysed/identified. No marked responses were observed for the other metabolic classes, e.g. polyketides, terpene-phenolics, nitrogen-containing secondary compounds and xanthones. Regarding the number of compounds significantly modulated by the UV-B radiation (Fig. 3C-D), the terpenoid class showed the greatest number of compounds affected by the UV-B exposure, with 52 and 112 terpenoids after 24 h and 36 h, respectively. The second most affected metabolic class was the phenylpropanoid derivatives, which included 29 compounds in the 24 h recovery and 62 compounds in the 36 h recovery samples. Together, terpenoids and phenylpropanoids derivatives covered 70% and 67% of the total number of significantly affected compounds considering the 24 h and 36 h recovery time, respectively, showing the high responsiveness of such metabolic classes towards UV-B radiation. Furthermore, it is interesting to notice that more than twice as much metabolites were identified in the Volcano analysis after 36 h compared to the number of metabolites after 24 h (116 compounds

306 in 24 h recovery, while 258 compounds in 36 h recovery). Thus, the UV-B exposure induced
307 metabolomic changes in peach flesh became more visible 36 h after the UV-B exposure.
308 A rearrangement in the metabolite pattern has been already observed in peach skins after both 10
309 min and 60 min UV-B treatments, which was correlated to the recovery time points (Santin et al.,
310 2018a). Particularly, a parallelism between peach skin and flesh can be observed in terms of number
311 of differential compounds detected according to the Volcano analysis. In fact, a higher number of
312 significantly induced compounds was detected after 36 h for both treatments also in the skin (4
313 compounds after 24 h and more than 20 after 36 h), indicating that UV-B-induced biochemical
314 effects are mainly visible after a recovery period of several hours after the irradiation, both in skin
315 and flesh. This might be probably due to the time needed to activate the biosynthetic genes after the
316 UV-B signalling pathway is triggered, and to synthesize and accumulate the metabolites.
317 Furthermore, 36 h after the UV-B treatment, the main responsive metabolite classes were the same
318 as observed in peach skin by Santin et al. (2018a), which were phenolics, terpenoids and lipids,
319 underlying a great similarity in the UV-B-responsiveness between the two fruit tissues.
320
321 **3.4 UV-B treatment differently influences the phenolic content according to each subclass**
322 **and recovery time point in peach flesh**
323 The effect of the UV-B treatment on the phenolic class was strongly influenced by both the UV-B
324 dose and the recovery time (Fig. 4). Moreover, the UV-B irradiation differently affected the
325 phenolic concentration according to each phenolic subclass. Indeed, in the 24 h recovery (Fig. 4A),
326 a general decrease was observed for both the 10 and the 60 min UV-B treatments. In contrast, 36 h
327 after the irradiation (Fig. 4B), both UV-B treatments induced an overall accumulation of most
328 phenolic subclasses. Interestingly, when the whole set of phenolic subclasses is considered, a
329 similarity in the UV-B response can be detected between the peach flesh and skin. Santin et al.
330 (2018a) reported a general downregulation of most of phenolics in the peach skin after 24 h and
331 hypothesized that the phenolics are probably consumed after the UV-B-induced oxidative stress.

The overall accumulation detected 36 h after the irradiation is most likely due to the UV-B-induced activation of the phenylpropanoid biosynthetic genes (e.g. *CHS*, *F3H*, *F3'H*, *DFR*) (Santin et al., 2019b). Such up-and-down trend has been also observed in peach flesh, although the responses according to each phenolic subclass might vary between tissues.

More specifically, regarding the 24 h recovery time point (Fig. 4A), the 10 min UV-B exposure was effective in increasing the concentration especially of carboxylic esters (+6.18 log_2FC) and β-diketones (+4.44 log_2FC), while the main subclasses undergoing a decrease were pterocarpans (-4.35 log_2FC) and stilbenes (-3.64 log_2FC). Considering the 60 min UV-B exposure, an increase was observed especially for flavonols (+7.99 log_2FC) and anthocyanins (+4.16 log_2FC), while the phenolic subclasses undergoing a decrease were mainly phenylpropenes (-8.08 log_2FC), isoflavonoids (-5.94 log_2FC), chalcones (-3.49 log_2FC), flavones (-3.21 log_2FC) and quinones (-3.21 log_2FC). The 36 h recovery time point (Fig. 4B) had a more complex scenario. More phenolic subclasses were identified, suggesting a stronger and more visible effect of both the UV-B exposures.

The decreased phenolics in the 10 min UV-B exposed samples were β-diketones (-7.44 log_2FC), benzoyl glycosides (-6.56 log_2FC), hydroxycinnamic acids (-5.13 log_2FC) and anthocyanins (-3.30 log_2FC), while the ones that increased were especially flavonols (+14.54 log_2FC), flavones (+11.32 log_2FC), quinones (+7.28 log_2FC) and flavanones (+5.08 log_2FC). In the 60 min UV-B-treatment, the class of β-diketones was the most decreased subclass identified (-4.49 log_2FC), but a slight decrease was also observed for anthocyanins (-0.42 log_2FC), amino acids (-0.57 log_2FC), flavonols (-1.04 log_2FC) and stilbenes (-0.37 log_2FC). However, the same UV-B exposure induced a noteworthy accumulation of much more phenolic subclasses, particularly flavones (+14.67 log_2FC), flavanones (+10.07 log_2FC), chalcones (+10.60 log_2FC) and phenylpropenes (+10.48 log_2FC).

Significant modulations of several anthocyanins, flavonols and flavones occurred also in peach skin (Santin et al., 2018a; Santin, et al., 2019b), probably due to their great antioxidant properties necessary to counteract the UV-B-induced oxidative stress. However, the behaviour of such

phenolic subclasses differed between the flesh and the skin. Indeed, anthocyanins and flavones concentration decreased in the skin after 24 h for both the 10 and 60 min UV-B treatments, followed by a great increase after 36 h (Santin et al., 2018a). Flavones showed a similar behaviour also in the flesh, with a UV-B dose-dependent response. However, the trend of anthocyanins differed significantly between the two tissues. Flesh anthocyanins, in fact, reacted to UV-B irradiation by increasing in the 60 min UV-B-treated samples after 24 h and decreasing 36 h after both the irradiations. Flavonols, which decreased in both recovery times and for both UV-B treatments in the peach skin, strongly increased 24 h and 36 h after the 10 min and 60 min UV-B treatment in the peach flesh. Although with different peach cultivars and applying different UV-B doses, a significant modulation in phenolic pattern of peach skin has also been observed in previous experiments. Indeed, Scattino et al. (2014) found that a 24 h UV-B exposure induced an accumulation of many flavonols glycosides, as well as of the cyanidin-3-glucoside, in "Suncrest" peaches. Contrarily, a decrease in hydroxycinnamic acids, the chlorogenic acid, the neochlorogenic acid and the cryptochlorogenic acid, was detected when peaches were UV-B-treated for 12 h and 24 h.

In terms of the number of compounds for each phenolic subclass, 24 h after the treatments (Fig. 4C), the flavonol subclass included the highest number of significantly UV-B-affected members (4), followed by carboxylic esters, flavones and isoflavonoids, with 3 metabolites per subclass. Flavonols represented the most responsive class also 36 h after the irradiation (Fig.4D), including 7 differentially accumulated metabolites followed by chalcones, flavones, hydroxycinnamic acids and lignans presented several UV-B-affected compounds (5).

3.5 UV-B irradiation affects terpenoid profile in peach flesh

Terpenoids represent a wide metabolite class within the plant kingdom with multiple functions for plant development and for humans after consumption. They largely contribute to the organoleptic properties of fruit and plant-based food in general, determining their commercial quality and

384 consumers' acceptance (Liu et al., 2017). Moreover, depending on the terpenoid subclasses and
385 compounds, they can also provide several benefits for human health, contributing to the prevention
386 of diseases, e.g. several types of cancers, diabetes and enteric pathogen infections (Khan,
387 Khundmiri, Khundmiri, Al-Sanea & Mok, 2018).
388 In this work, terpenoids were influenced by the UV-B radiation, with differences among each
389 subclass mainly due to the recovery time (Fig. 5). At the 24 h recovery time point (Fig. 5A), most
390 terpenoid classes detected in the volcano analysis underwent a decrease. Specifically, the
391 diterpenoids were the most affected subclass, with a -16.85 and a -46.62 log_2FC decrease in the 10
392 min and 60 min UV-B treatment samples, respectively. Besides the diterpenoids, UV-B exposure
393 was effective also in reducing the concentration of sterols (-17.27 and -12.45 log_2FC in the 10 min
394 and 60 min UV-B-treated samples, respectively) and triterpenoids (-8.20 and -18.05 log_2FC in the
395 10 min and 60 min UV-B treatment samples, respectively). A slight decrease was observed also for
396 sesquiterpenoids and monoterpenoids in the 60 min UV-B-treated samples (-2.51 and -0.38 log_2FC,
397 respectively). Contrarily, carotenoids strongly accumulated in the 60 min UV-B samples, with a
398 +33.41 log2FC increase, although they were decreased in the 10 min UV-B samples (a -3.01
399 log_2FC). Finally, the 60 min UV-B-treatment resulted in an accumulation of sesterpenoids 24 h after
400 the UV-B exposure, while no effects were observed when peaches were treated for 10 min.
401 After 36 h recovery (Fig. 5B), an overall accumulation of all the terpenoid subclasses was detected
402 in UV-B-treated samples, except for the sequiterpenoids in the 60 min UV-B-treated samples and
403 the triterpenoids in the 10 min UV-B-treated samples, which underwent a -4.77 and a -4.19 log_2FC
404 decrease, respectively. The terpenoid subclasses with the greatest increase were the carotenoids, the
405 diterpenoids and the triterpenoids in the 60 min UV-B-treated fruit, with an accumulation of
406 +47.33, +38.82 and +30.10 log_2FC, respectively.
407 Regarding the number of terpenoids for each subclass detected in the Volcano analysis, the most
408 responsive classes 24 h after UV-B treatment (Fig. 5C) were carotenoids, diterpenoids and
409 triterpenoids, with 16, 14 and 10 significantly affected compounds, respectively. In the 36-h

410 recovery time (Fig. 5D) however, the sesquiterpenoids showed the highest number of differentially
411 accumulated compounds (46), followed by carotenoids (20) and triterpenoids (18). The current
412 literature reports only very few analyses of UV-B effect on the terpenoid class in peach fruit. Liu et
413 al. (2017) have found that 48 h UV-B irradiation decreased the concentration of linalool, which
414 highly contributes to the characteristic peach flavour, but increased the concentration of (*E*, *E*)-α-
415 farnesene, which plays a key role in defence against biotic stresses. In addition, Santin et al. (2018a)
416 have also found an UV-B-induced modulation of terpenoids in peach skin. Among terpenoids,
417 carotenoids play a fundamental role in terms of peach quality, since they contribute to the fruit
418 colour and guide consumers' preferences towards certain cultivars. Furthermore, some carotenoids,
419 e.g. β-carotene, α-carotene, and β-cryptoxanthin, besides providing benefits for human health due to
420 their antioxidant properties, are well-known precursors of vitamin A (Caprioli, Lafuente, Rodrigo &
421 Mencarelli, 2009). Thus, a postharvest UV-B treatment able to enhance the accumulation of such
422 secondary metabolites might determine an increase in the nutraceutical value of the UV-B-exposed
423 fruit, increasing their overall quality. In addition, terpenoids have been described to counteract
424 biotic and abiotic stresses (Yazaki, Arimura & Ohnishi, 2017), so a UV-B-driven increase in
425 terpenoids content might protect the fruit towards many environmental factors that can occur during
426 the processing and distribution steps.
427
428 **3.6 UV-B radiation does not penetrate peach skin**
429 Once elucidated that UV-B exposure is effective in modulating the secondary metabolites also in
430 the peach flesh, and particularly for the phenolic and terpenoid classes, the most direct question
431 arising from this observation deals with understanding whether the UV-B radiation can penetrate
432 the peach skin. This way, it is possible to unravel if the biochemical effects observed are due to a
433 direct irradiation of the flesh, or if some chemical/physical signalling interplays between the UV-B-
434 exposed skin and the flesh underneath. Peach fruit used for this analysis were at the same stage as
435 the UV-B-irradiated ones, which was "ready to buy" (Valero, Crisosto and Slaughter, 2007; Santin

et al., 2019a), to avoid any differences in light transmittance due to different ripening stages. The results of spectrophotometric transmittance analysis of the peach skin are shown in Fig. 6. Since the colour of peach skin of different cultivars varies from yellow to dark red, and since the different pigmentation might have different light absorption properties, this analysis was performed across dark red, bright red and yellow skin portions. As represented in Fig. 6A, the percentage of transmittance (%T) is strictly dependent on the peach skin colour. Indeed, the darker the skin is, the lower is the %T in the interval between 320 nm to 640-660 nm. Interestingly, the light across both yellow and bright red skins starts to penetrate to a very low extent from around 325 nm (Fig. 6B), while the dark red skin completely absorbs radiations wavelengths below 340 nm This means that light transmittance begins in the UV-A range (315-400 nm). Taking into account that the UV-B wavelength interval is 280-315 nm, these results reveal that none of the peach skin tested, regardless of the colour, let the UV-B radiation pass through.

In light of this, it is reasonable to assume that flesh tissue, which is totally UV-B-shielded by the skin above, did not incur the strong decrease of phenolics observed in the peach skin, which occurred especially for flavones, anthocyanins and dihydroflavonols (Santin et al. 2018a). Such decrease in the content of phenolics was explained as a consumption of antioxidant compounds to counteract a potentially damaging UV-B-induced oxidative stress. However, since the UV-B radiation does not hit directly the peach flesh underneath, it is highly probable that the reduced decrease of phenolics was due to a scarce production of ROS. Nevertheless, a strong overall increase of phenolics was observed after 36 h the UV-B irradiation, similarly to what was reported in the skin by Santin et al. (2018a). UV-B-induced overexpression of phenylpropanoid biosynthetic genes, e.g. *chalcone synthase* (*CHS*), *chalcone isomerase* (*CHI*), *flavanone 3-hydroxylase* (*F3H*), *dihydroflavonol 4-reductase* (*DFR*), *anthocyanidin synthase* (*ANS*) was already studied in many fruit species (Catola et al., 2017; Santin et al., 2019b; Scattino et al., 2014; Ubi et al., 2006; Zhao et al., 2017) which might have induced the strong accumulation of phenolics in the peach skin mentioned above. However, for the UV-B-shielded fruit tissues, such as the flesh, no literature data

were reported. Our results indicate that a signalling mechanism might occur between the outer, and UV-B-exposed, skin and the inner flesh, which might have determined the metabolomic changes discussed in this work. Santin et al. (2018a) reported a possible UV-B-induced lipid peroxidation in the peach skin, with the consequent formation of short-chained cleavage products that might act as secondary messengers through membranes and different tissues. Similarly, also UV-B-induced ROS, which are reported to increase in UV-B-exposed tissues (Czégény, Mátai & Hideg, 2016) might have migrated in tissues, inducing changes in the metabolomic profile also in the UV-B-shielded flesh, without reaching the toxicity threshold level. The hypothesis of UV-B-related messengers across fruit tissues is highly supported by the results of this work, and surely deserves deeper studies.

4. CONCLUSIONS

Although the current literature about UV-B-driven metabolomic effects on fruit almost exclusively focuses on the skin or the whole fruit, this work showed that the UV-B exposure, depending on the UV-B dose and the recovery time, is able to strongly impact the metabolome also in the peach flesh. Both the UV-B doses induced a general decrease in almost all the metabolic classes, especially terpenoids, phytoalexins and phenylpropanoid derivatives, 24 h after the exposure. However, after 36 h, an overall increase of the same metabolite classes was detected, with a stronger effect for the 60 min UV-B treatment, suggesting a dose-dependent effect of the UV-B exposure. The same trend was observed also for individual phenolic subclasses, which was similar to the trend shown of the phenolics in the UV-B-exposed skin tissue. This work also gives evidence that, despite the noteworthy metabolomic changes, the UV-B radiation does not penetrate the fruit skin, suggesting a possible UV-B-related signalling pathway between tissues. Since most consumers use to peel peach fruit before eating it, the great potential of UV-B radiation to increase the nutraceutical value of the UV-B-shielded flesh tissue underneath deserves a particular attention. When it comes to fruit quality, according to Santin et al. (2019a), both 10-min and 60-min UV-B treatments did not

488 influence the titratable acidity nor the soluble solid content of peach fruit. However, they were
489 effective in reducing the loss of firmness after 24 h from the 60-min UV-B irradiation. Moreover, In
490 the light of the great modifications observed also among terpenoids, next steps will be to investigate
491 whether such changes might influence the organoleptic properties of peach fruit. In this sense,
492 further analyses, e.g. colour measurements, aromatic profiling and panel tests, will be certainly
493 performed in order to evaluate the impact of UV-B-treated fruit among consumers. In addition, the
494 possible migration of UV-B-induced molecules from the skin to the flesh, able to induce such
495 metabolomic variations, will be deepen further.
496

497 ## 5. ACKNOWLEDGEMENTS

498 The research was supported by funds of the University of Pisa and by a grant of the Austrian
499 Science Fund FWF I 1725-B16. MS carried out part of the present work in M-TH's labs, at the
500 Department of Applied Genetics and Cell Biology, University of Natural Resources and Life
501 Sciences, supported by a grant for a post-degree Erasmus+ traineeship. ÅS was supported by grants
502 from the Knowledge foundation (kks.se; contract no. 20130164), The Swedish Research Council
503 Formas (formas.se/en; Contract no. 942-2015-516), by Örebro University's Faculty for Business,
504 Science and Technology, and the Örebro University's Strategic Research Program 'Food and
505 Health'. We kindly acknowledge the technical support of Julia Richter and Nataliia Konstantinova
506 for help with the sampling.
507

508 ## 6. REFERENCES

509 Acosta-Estrada, B. A., Gutiérrez-Uribe, J. A., & Serna-Saldívar, S. O. (2014). Bound phenolics in
510 foods, a review. *Food Chemistry, 152*, 46–55. https://doi.org/10.1016/j.foodchem.2013.11.093
511 Agatonovic-Kustrin, S., Kustrin, E., & Morton, D. W. (2018). Phenolic acids contribution to
512 antioxidant activities and comparative assessment of phenolic content in mango pulp and peel.
513 *South African Journal of Botany, 116*, 158–163. https://doi.org/10.1016/j.sajb.2018.03.013

514 Assumpção, C. F., Hermes, V. S., Pagno, C., Castagna, A., Mannucci, A., Sgherri, C., Pinzino, C.,
515 Ranieri, A., Flôres, S. H., & Rios, A. de O. (2018). Phenolic enrichment in apple skin
516 following post-harvest fruit UV-B treatment. *Postharvest Biology and Technology, 138*, 37-45.
517 https://doi.org/10.1016/j.postharvbio.2017.12.010
518 Camejo, D., Guzmán-Cedeño, Á., & Moreno, A. (2016). Reactive oxygen species, essential
519 molecules, during plant-pathogen interactions. *Plant Physiology and Biochemistry*, *103*, 10–
520 23. https://doi.org/10.1016/j.plaphy.2016.02.035
521 Caprioli, I., Lafuente, M. T., Rodrigo, M. J., & Mencarelli, F. (2009). Influence of postharvest
522 treatments on quality, carotenoids, and abscisic acid content of stored "spring belle" peach
523 (*Prunus persica*) fruit. *Journal of Agricultural and Food Chemistry*, *57*(15), 7056–7063.
524 https://doi.org/10.1021/jf900565g
525 Castagna, A., Dall'Asta, C., Chiavaro, E., Galaverna, G., & Ranieri, A. (2014). Effect of post-
526 harvest UV-B irradiation on polyphenol profile and antioxidant activity in flesh and peel of
527 tomato fruits. *Food and Bioprocess Technology*, *7*(8), 2241–2250.
528 https://doi.org/10.1007/s11947-013-1214-5
529 Catola, S., Castagna, A., Santin, M., Calvenzani, V., Petroni, K., Mazzucato, A., & Ranieri, A.
530 (2017). The dominant allele *Aft* induces a shift from flavonol to anthocyanin production in
531 response to UV-B radiation in tomato fruit. *Planta*, *246*(2), 263–275.
532 https://doi.org/10.1007/s00425-017-2710-z
533 Cheynier, V., Comte, G., Davies, K. M., Lattanzio, V., & Martens, S. (2013). Plant phenolics:
534 Recent advances on their biosynthesis, genetics, andecophysiology. *Plant Physiology and*
535 *Biochemistry, 72*, 1–20. https://doi.org/10.1016/j.plaphy.2013.05.009
536 Choudhury, F. K., Rivero, R. M., Blumwald, E., & Mittler, R. (2017). Reactive oxygen species,
537 abiotic stress and stress combination. *Plant Journal*, *90*(5), 856–867.
538 https://doi.org/10.1111/tpj.13299
539 Czégény, G., Mátai, A., & Hideg, É. (2016). UV-B effects on leaves-Oxidative stress and

acclimation in controlled environments. *Plant Science*, *248*, 57–63. https://doi.org/10.1016/j.plantsci.2016.04.013

Dreyer, A., & Dietz, K.-J. (2018). Reactive oxygen species and the redox-regulatory network in cold stress acclimation. *Antioxidants*, *7*(11), 169. https://doi.org/10.3390/antiox7110169

Eggersdorfer, M., & Wyss, A. (2018). Carotenoids in human nutrition and health. *Archives of Biochemistry and Biophysics*, *652*, 18-26. https://doi.org/10.1016/j.abb.2018.06.001

Feeney, J., Finucane, C., Savva, G. M., Cronin, H., Beatty, S., Nolan, J. M., & Kenny, R. A. (2013). Low macular pigment optical density is associated with lower cognitive performance in a large, population-based sample of older adults. *Neurobiology of Aging*, *34*(11), 2449–2456. https://doi.org/10.1016/j.neurobiolaging.2013.05.007

Gomes, T. M., Toaldo, I. M., Haas, I. C. da S., Burin, V. M., Caliari, V., Luna, A. S., de Gois, J. S., & Bordignon-Luiz, M. T. (2019). Differential contribution of grape peel, pulp, and seed to bioaccessibility of micronutrients and major polyphenolic compounds of red and white grapes through simulated human digestion. *Journal of Functional Foods*, *52*, 699–708. https://doi.org/10.1016/j.jff.2018.11.051

Corpas, F. J., Gupta, D. K., & Palma, J. M. (2015). Production sites of reactive oxygen species (ROS) in organelles from plant cells. In Gupta, D. K., Palma, J. M., & Corpas, F. J. (Eds.), *Reactive oxygen species and oxidative damage in plants under stress* (pp. 1-22). Heidelberg: Springer.

Hideg, É., Jansen, M. A. K., & Strid, Å. (2013). UV-B exposure, ROS, and stress: Inseparable companions or loosely linked associates? *Trends in Plant Science*, *18*(2), 107–115. https://doi.org/10.1016/j.tplants.2012.09.003

Jansen, M. A. K., Gaba, V., & Greenberg, B. M. (1998). Higher plants and UV-B radiation: balancing damage, repair and acclimation. *Trends in Plant Science*, *3*(4), 131–135. https://doi.org/10.1016/S1360-1385(98)01215-1

Jansen, M. A. K., Hectors, K., O'Brien, N. M., Guisez, Y., & Potters, G. (2008). Plant stress and

566 human health: Do human consumers benefit from UV-B acclimated crops? *Plant Science*,
567 *175*(4), 449-458. https://doi.org/10.1016/j.plantsci.2008.04.010
568 Karp, P. D., Paley, S. M., Krummenacker, M., Latendresse, M., Dale, J. M., Lee, T. J., Kaipa, P.,
569 Gilham, F., Spaulding, A., Popescu, L., Altman, T., Paulsen, I., Keseler I. M., & Caspi, R.
570 (2010). Pathway Tools version 13.0: integrated software for pathway/genome informatics and
571 systems biology. *Briefings in bioinformatics*, *11*(1), 40-79. https://doi.org/10.1093/bib/bbp043
572 Khan, M. S. A., Khundmiri, S. U. K., Khundmiri, S. R., Al-Sanea, M. M., & Mok, P. L. (2018).
573 Fruit-derived polysaccharides and terpenoids: Recent update on the gastroprotective effects
574 and mechanisms. *Frontiers in Pharmacology*, *9*, 569. https://doi.org/10.3389/fphar.2018.00569
575 Kokalj, D., Bizjak, G., Zlatić, E., Cigić, B., Hribar, J., & Vidrih, R. (2016). Influence of UV-B light
576 emitting diodes on colour development and accumulation of polyphenols and antioxidants in
577 apple skin. *Agriculturae Conspectus Scientificus*, *81*(3).
578 Kopsell, D. A., & Kopsell, D. E. (2006). Accumulation and bioavailability of dietary carotenoids in
579 vegetable crops. *Trends in Plant Science*, *11*(10), 499–507.
580 https://doi.org/10.1016/j.tplants.2006.08.006
581 Lee, J., Chan, B. L. S., & Mitchell, A. E. (2017). Identification/quantification of free and bound
582 phenolic acids in peel and pulp of apples (*Malus domestica*) using high resolution mass
583 spectrometry (HRMS). *Food Chemistry*, *215*, 301–310.
584 https://doi.org/10.1016/j.foodchem.2016.07.166
585 Lee, M. J., Son, J. E., & Oh, M. M. (2014). Growth and phenolic compounds of *Lactuca sativa* L.
586 grown in a closed-type plant production system with UV-A, -B, or -C lamp. *Journal of the*
587 *Science of Food and Agriculture*, *94*(2), 197–204. https://doi.org/10.1002/jsfa.6227
588 Liu, H., Cao, X., Liu, X., Xin, R., Wang, J., Gao, J., Wu, B., Gao, L., Xu, C., Zhang, B., Grierson,
589 D., & Chen, K. (2017). UV-B irradiation differentially regulates terpene synthases and terpene
590 content of peach. *Plant Cell and Environment*, *40*(10), 2261–2275.
591 https://doi.org/10.1111/pce.13029

592 Nunez, M., Forgan, B., & Roy, C. (1994). Estimating ultraviolet radiation at the earth's surface.
593 *International Journal of Biometeorology*, *38*(1), 5–17. https://doi.org/10.1007/BF01241798
594 Rizzini, L., Favory, J. J., Cloix, C., Faggionato, D., O'Hara, A., Kaiserli, E., Baumeister, R.,
595 Schäfer, E., Nagy, F., Jenkins, G. I., & Ulm, R. (2011). Perception of UV-B by the arabidopsis
596 UVR8 protein. *Science*, *332*(6025), 103–106. https://doi.org/10.1126/science.1200660
597 Rodriguez-Concepcion, M., Avalos, J., Bonet, M. L., Boronat, A., Gomez-Gomez, L., Hornero-
598 Mendez, D., Limon, M. C., Meléndez-Martínez, A. J., Olmedilla-Alonso, B., Palou, A., Ribot,
599 J., Rodrigo, M. J., Zacarias, L., & Zhu, C. (2018). A global perspective on carotenoids:
600 Metabolism, biotechnology, and benefits for nutrition and health. *Progress in Lipid Research*,
601 *70*, 62–93. https://doi.org/10.1016/j.plipres.2018.04.004
602 Saidani, F., Giménez, R., Aubert, C., Chalot, G., Betrán, J. A., & Gogorcena, Y. (2017). Phenolic,
603 sugar and acid profiles and the antioxidant composition in the peel and pulp of peach fruits.
604 *Journal of Food Composition and Analysis*, *62*, 126-133.
605 https://doi.org/10.1016/j.jfca.2017.04.015
606 Santin, M., Lucini, L., Castagna, A., Chiodelli, G., Hauser, M.-T., & Ranieri, A. (2018a). Post-
607 harvest UV-B radiation modulates metabolite profile in peach fruit. *Postharvest Biology and*
608 *Technology*, *139*, 127–134. https://doi.org/10.1016/j.postharvbio.2018.02.001
609 Santin, M., Giordani, T., Cavallini, A., Bernardi, R., Castagna, A., Hauser, M.-T., & Ranieri, A.
610 (2019a). UV-B exposure reduces the activity of several cell wall-dismantling enzymes and
611 affects the expression of their biosynthetic genes in peach fruit (*Prunus persica* L., cv.
612 Fairtime, melting phenotype). *Photochemical & Photobiological Sciences*, *18*(5), 1280-1289.
613 https://doi.org/10.1039/C8PP00505B
614 Santin, M., Lucini, L., Castagna, A., Rocchetti, G., Hauser, M. T., & Ranieri, A. (2019b).
615 Comparative "phenol-omics" and gene expression analyses in peach (*Prunus persica*) skin in
616 response to different postharvest UV-B treatments. *Plant Physiology and Biochemistry*, *135*,
617 511–519. https://doi.org/10.1016/j.plaphy.2018.11.009

618 Scattino, C., Castagna, A., Neugart, S., Chan, H. M., Schreiner, M., Crisosto, C. H., Tonutti, P., &
619 Ranieri, A. (2014). Post-harvest UV-B irradiation induces changes of phenol contents and
620 corresponding biosynthetic gene expression in peaches and nectarines. *Food Chemistry*, *163*,
621 51–60. https://doi.org/10.1016/j.foodchem.2014.04.077
622 Shahidi, F., & Ambigaipalan, P. (2015). Phenolics and polyphenolics in foods, beverages and
623 spices: Antioxidant activity and health effects - A review. *Journal of Functional Foods*, *18*,
624 820–897. https://doi.org/10.1016/j.jff.2015.06.018
625 Sheng, K., Zheng, H., Shui, S. S., Yan, L., Liu, C., & Zheng, L. (2018). Comparison of postharvest
626 UV-B and UV-C treatments on table grape: Changes in phenolic compounds and their
627 transcription of biosynthetic genes during storage. *Postharvest Biology and Technology*, *138*,
628 74–81. https://doi.org/10.1016/j.postharvbio.2018.01.002
629 Ubi, B. E., Honda, C., Bessho, H., Kondo, S., Wada, M., Kobayashi, S., & Moriguchi, T. (2006).
630 Expression analysis of anthocyanin biosynthetic genes in apple skin: Effect of UV-B and
631 temperature. *Plant Science*, *170*(3), 571–578. https://doi.org/10.1016/j.plantsci.2005.10.009
632 Valdés, L., Cuervo, A., Salazar, N., Ruas-Madiedo, P., Gueimonde, M., & Gonzàles, S. (2015). The
633 relationship between phenolic compounds from diet and microbiota: impact on human health.
634 *Food & Function*, *6*(8), 2424–2439.
635 Valero, C., Crisosto, C. H., & Slaughter, D. (2007). Relationship between nondestructive firmness
636 measurements and commercially important ripening fruit stages for peaches, nectarines and
637 plums. *Postharvest Biology and Technology*, *44*(3), 248-253.
638 https://doi.org/10.1016/j.postharvbio.2006.12.014
639 Yamaguchi, M., & Uchiyama, S. (2003). Effect of Carotenoid on Calcium Content and Alkaline
640 Phosphatase Activity in Rat Femoral Tissues in Vitro: The Unique Anabolic Effect of β-
641 Cryptoxanthin. *Biological & Pharmaceutical Bulletin*, *26*(8), 1188–1191.
642 https://doi.org/10.1248/bpb.26.1188
643 Yazaki, K., Arimura, G. I., & Ohnishi, T. (2017). “Hidden” terpenoids in plants: Their biosynthesis,

localization and ecological roles. *Plant and Cell Physiology*, *58*(10), 1615–1621. https://doi.org/10.1093/pcp/pcx123

Zhao, Y., Dong, W., Wang, K., Zhang, B., Allan, A. C., Lin-wang, K., Chen, K., & Xu, C. (2017). Differential sensitivity of fruit pigmentation to ultraviolet light between two peach cultivars. *Frontiers in Plant Science*, *8*, 1552. https://doi.org/10.3389/fpls.2017.01552

649 **FIGURES CAPTIONS**

650 Fig. 1. Concentration of phenolic compounds in peach flesh expressed as (A) mg/kg F.W. and (B)
651 mg/fruit.

652

653 Fig. 2. Unsupervised hierarchical cluster analysis of metabolomic profiles of peach flesh samples
654 clustered by UV-B exposures (10 min and 60 min) and recovery times (24 h and 36 h). Fold-change
655 heat-maps of UHPLC-ESI/QTOF untargeted metabolomic profiling was used to create
656 dendrograms. Clustering and dendrograms were produced by choosing the Euclidean distance and
657 Ward's linkage rule.

658

659 Fig. 3. Fold-change-based metabolite modifications in UV-B-treated peach flesh at (A) 24 h and (B)
660 36 h recovery time points. A combination of analysis of variance and fold-change into Volcano Plot
661 (Bonferroni multiple testing correction, $P < 0.05$; fold-change cut-off=2; n=5 per treatment) was
662 applied to identify the most responsive metabolites (the full list is reported in Table S3). The
663 log_2FCs of the compounds belonging to the same metabolite class, according to the PlantCyc
664 classification, were added up to get the overall behaviour of each class. A pie chart referred to the
665 (C) 24-h and (D) 36-h recovery time points, indicating the number of significantly modulated
666 compounds per class according to the statistical analysis explained above.

667

668 Fig. 4. Fold-change-based phenylpropanoid derivatives modifications in UV-B-treated peach flesh
669 at (A) 24 h and (B) 36 h recovery time points. A combination of analysis of variance and fold-
670 change into Volcano Plot (Bonferroni multiple testing correction, $P < 0.05$; fold-change cut-off=2;
671 n=5 per treatment) was applied to identify the most responsive phenylpropanoid derivatives (the full
672 list is reported in Table S3). The log_2FCs of the resulting compounds belonging to the same
673 phenolic subclass, according to the PlantCyc classification, were added up to get the overall
674 behaviour of each phenolic subclass**.** A pie chart referred to the (C) 24-h and (D) 36-h recovery time

675 points, indicating the number of significantly modulated compounds per class according to the
676 statistical analysis explained above.
677
678 Fig. 5. Fold-change-based terpenoids modifications in UV-B-treated peach flesh at (A) 24 h and (B)
679 36 h recovery time points. A combination of analysis of variance and fold-change into Volcano Plot
680 (Bonferroni multiple testing correction, $P < 0.05$; fold-change cut-off=2; n=5 per treatment) was
681 applied to identify the most responsive terpenoids (the full list is reported in Table S3). The log_2FCs
682 of the resulting compounds belonging to the same terpenoid subclass, according to the PlantCyc
683 classification, were added up to get the overall behaviour of each phenolic subclass. A pie chart
684 referred to the (C) 24-h and (D) 36-h recovery time points, indicating the number of significantly
685 modulated compounds per class according to the statistical analysis explained above.
686
687 Fig. 6. Spectrophotometric transmittance of peach skin using Shimadzu UV1800 UV/VIS
688 spectrophotometer. A) A transmittance recorded for wavelengths between 250 nm and 790 nm and
689 B) a blow-up of transmittance between 300 and 340 nm. Percentage of transmittance was
690 determined for dark red and bright red skin of particolored peach and yellow skin from peach cv.
691 Fairtime.
692
693
694 **CAPTIONS OF SUPPLEMENTARY MATERIAL**
695 Fig. S1. Emission spectrum of the UV-B narrowband tubes (Philips Ultraviolet-B Narrowband, TL
696 20W/01 – RS, Koninklijke Philips Electronics, Eindhoven, The Netherlands) used in this study.
697
698 Fig. S2. Graphical representation of the experimental setup.
699

Table S1. Dataset of phenolic compounds from UHPLC-ESI/QTOF untargeted metabolomic profiling identified using the database from Phenol-Explorer 3.6, together with OPLS-DA prediction model and VIP selection method.

Table S2. Dataset of metabolites from UHPLC-ESI/QTOF untargeted metabolomic profiling identified using the database from PlantCyc 9.6.

Table S3. Metabolites resulting from the analysis of variance and fold-change (Bonferroni multiple testing correction, $P < 0.05$; fold-change cut-off=2; n=5 per treatment). Full list of compounds, together with the respective FC value (UV-B-treated vs control) and p-value, for each UV-B exposure and recovery time.

***Declaration of Interest Statement**

Declaration of interests

☒ The authors declare that they have no known competing financial interests or personal relationships that could have appeared to influence the work reported in this paper.

☐The authors declare the following financial interests/personal relationships which may be considered as potential competing interests:

Figure 1

Click here to download high resolution image

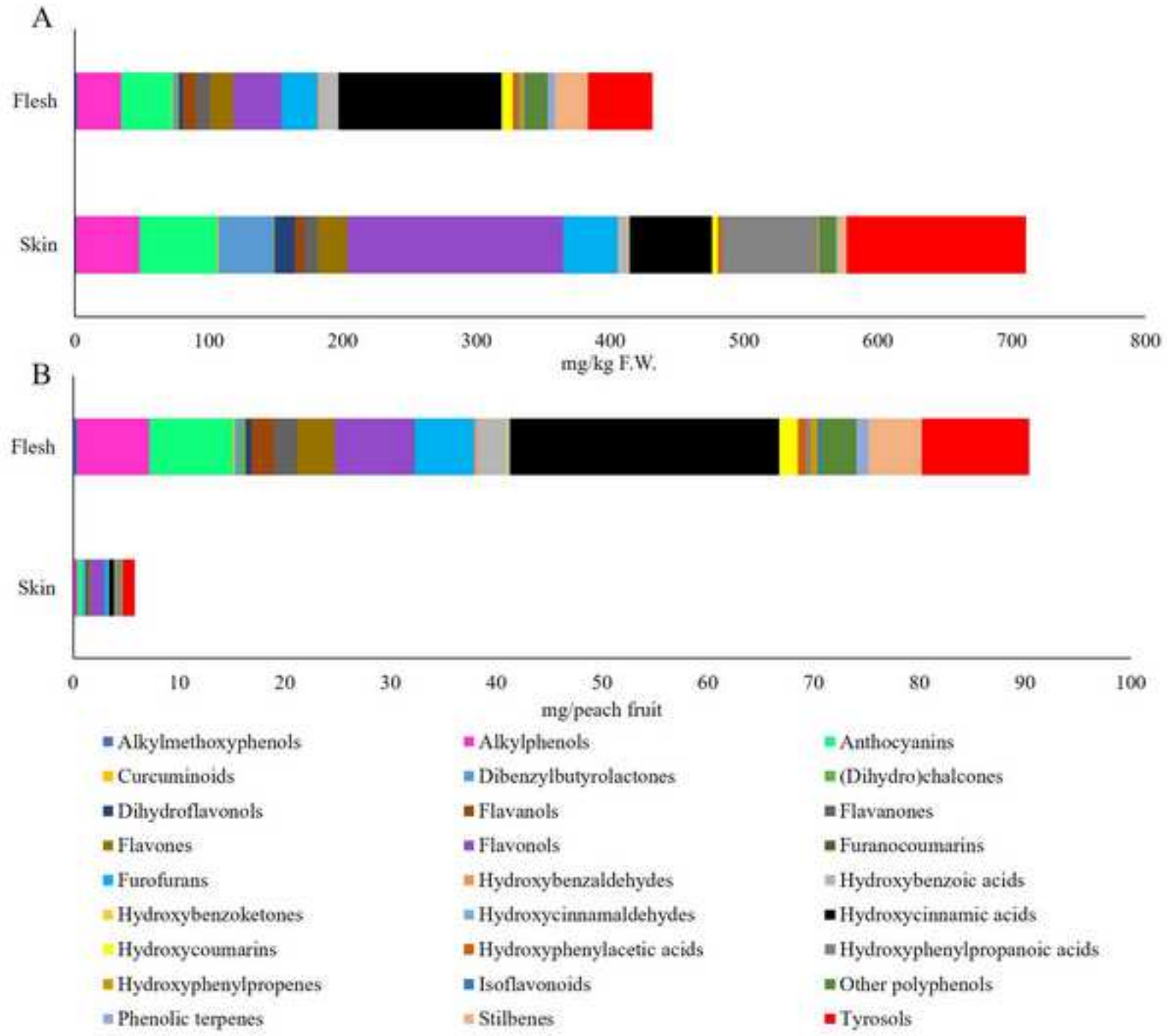

Figure 2

Click here to download high resolution image

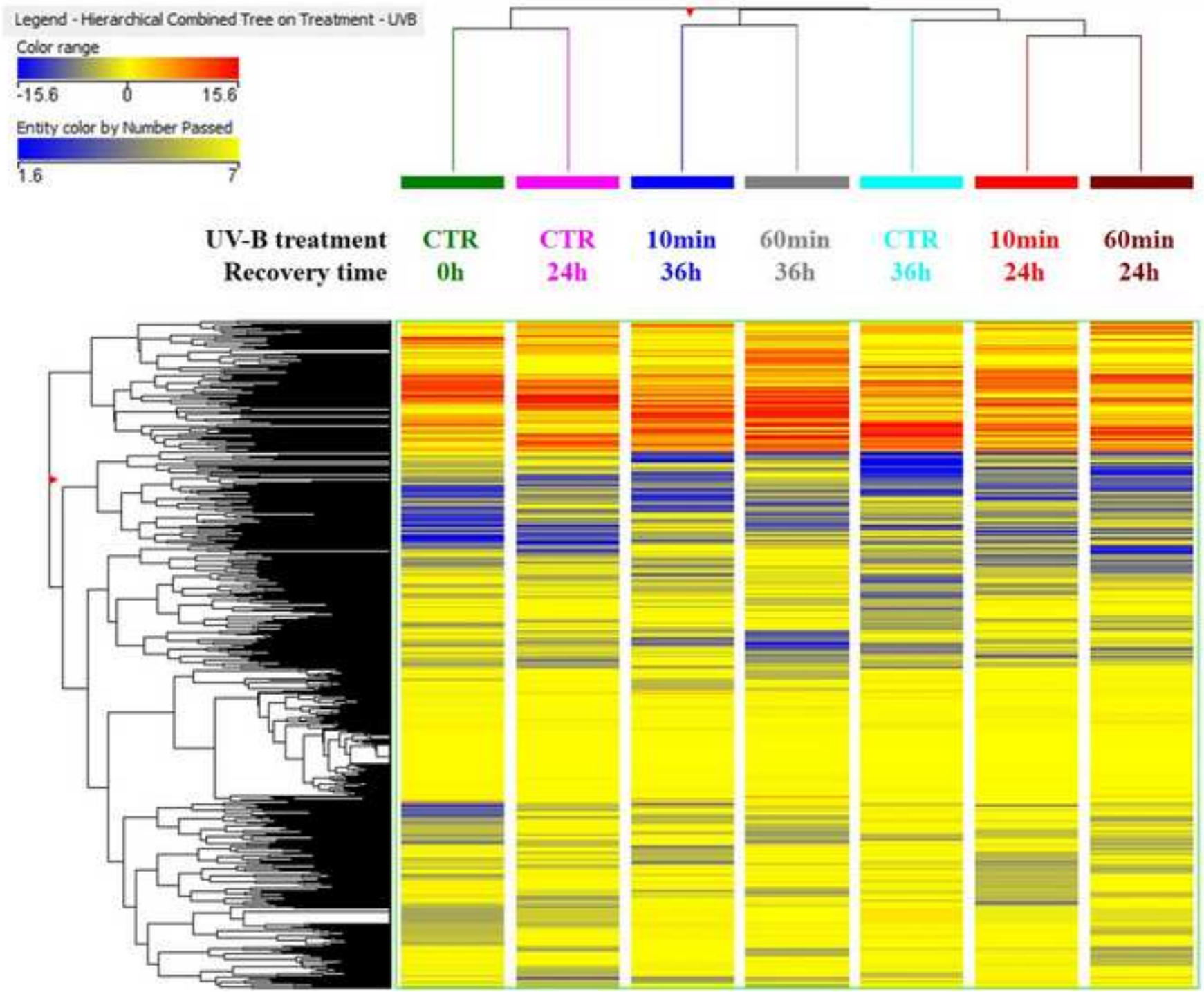

Figure 3

Click here to download high resolution image

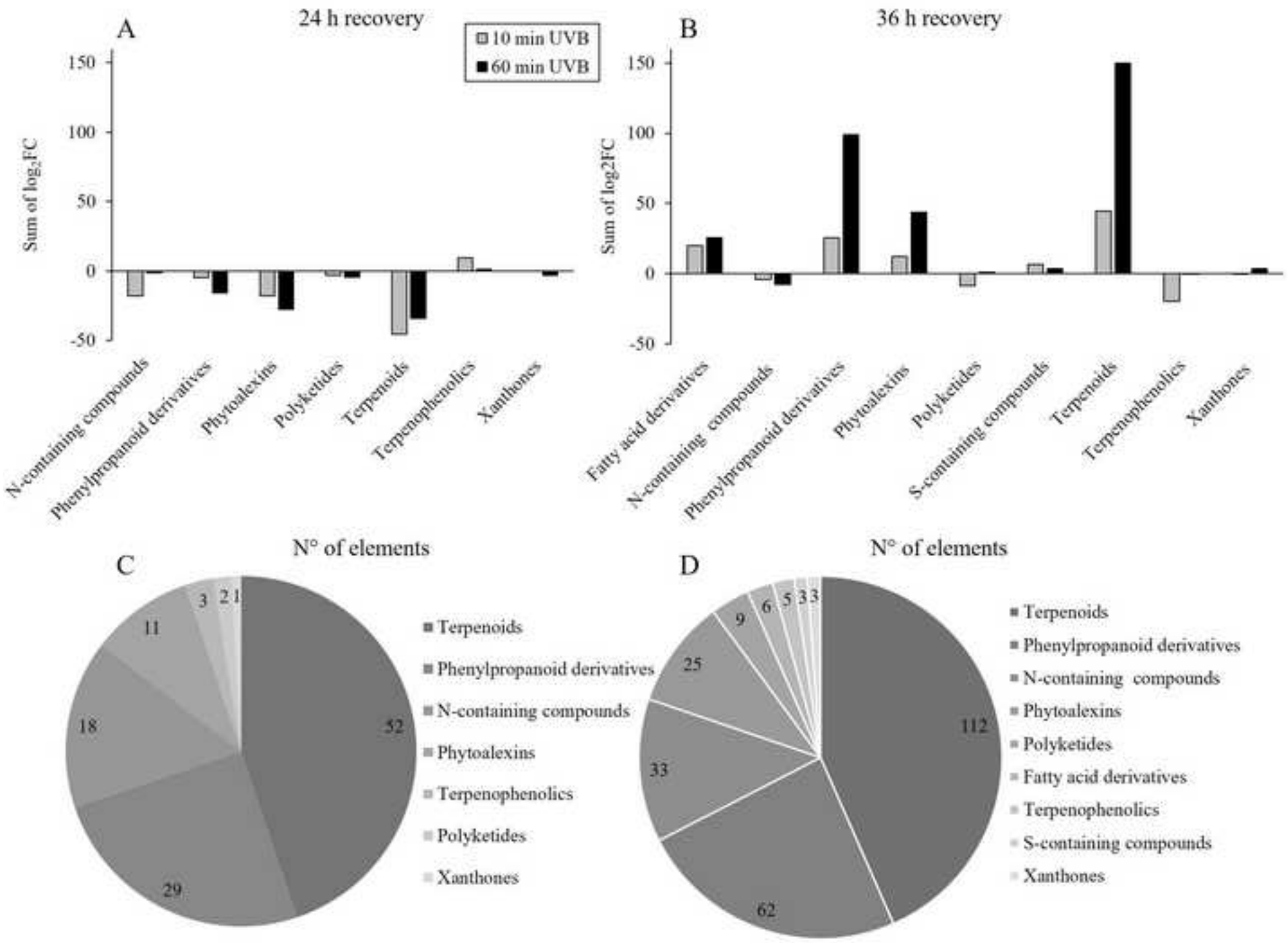

Figure 4

Click here to download high resolution image

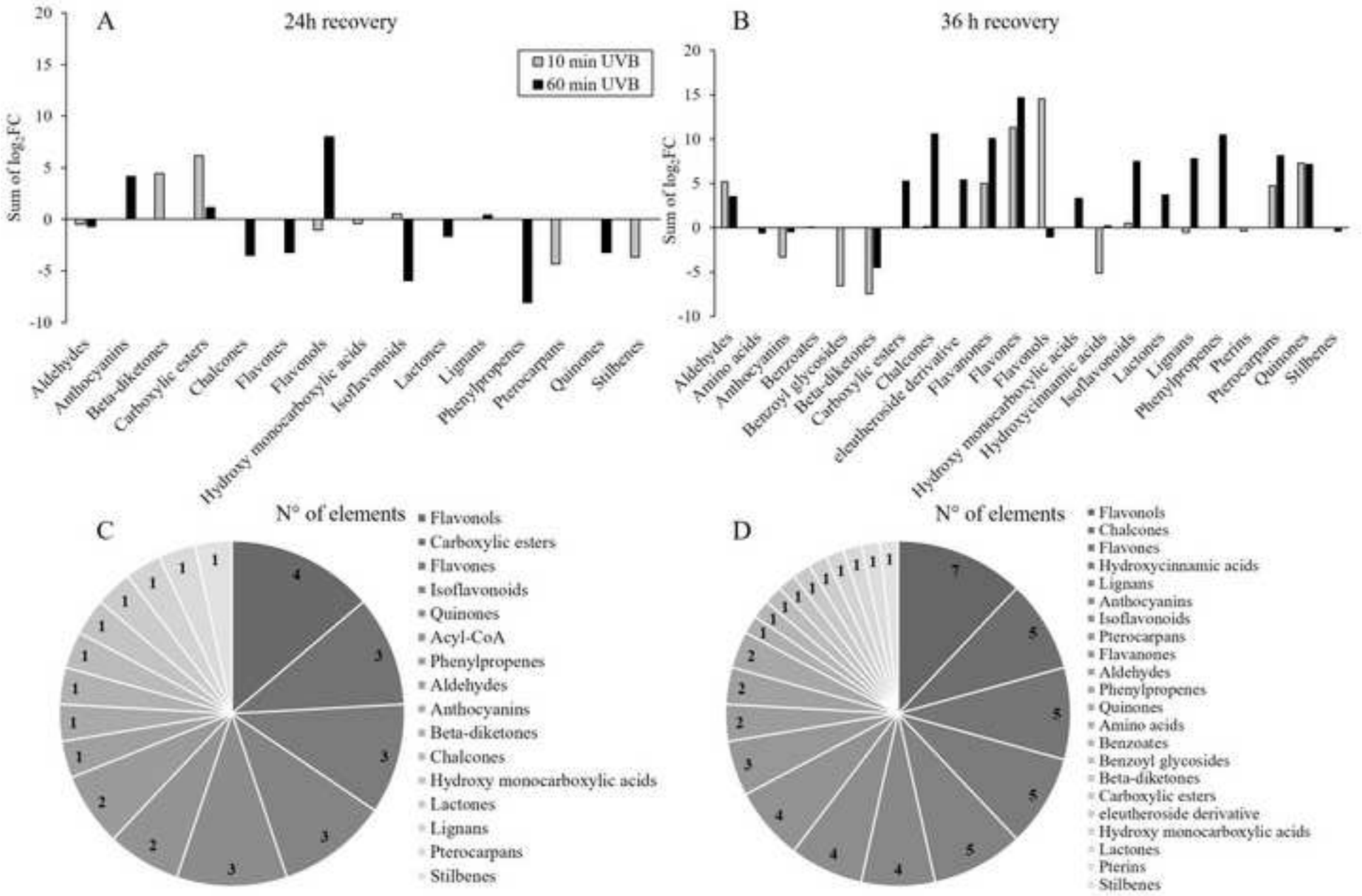

Figure 5

Click here to download high resolution image

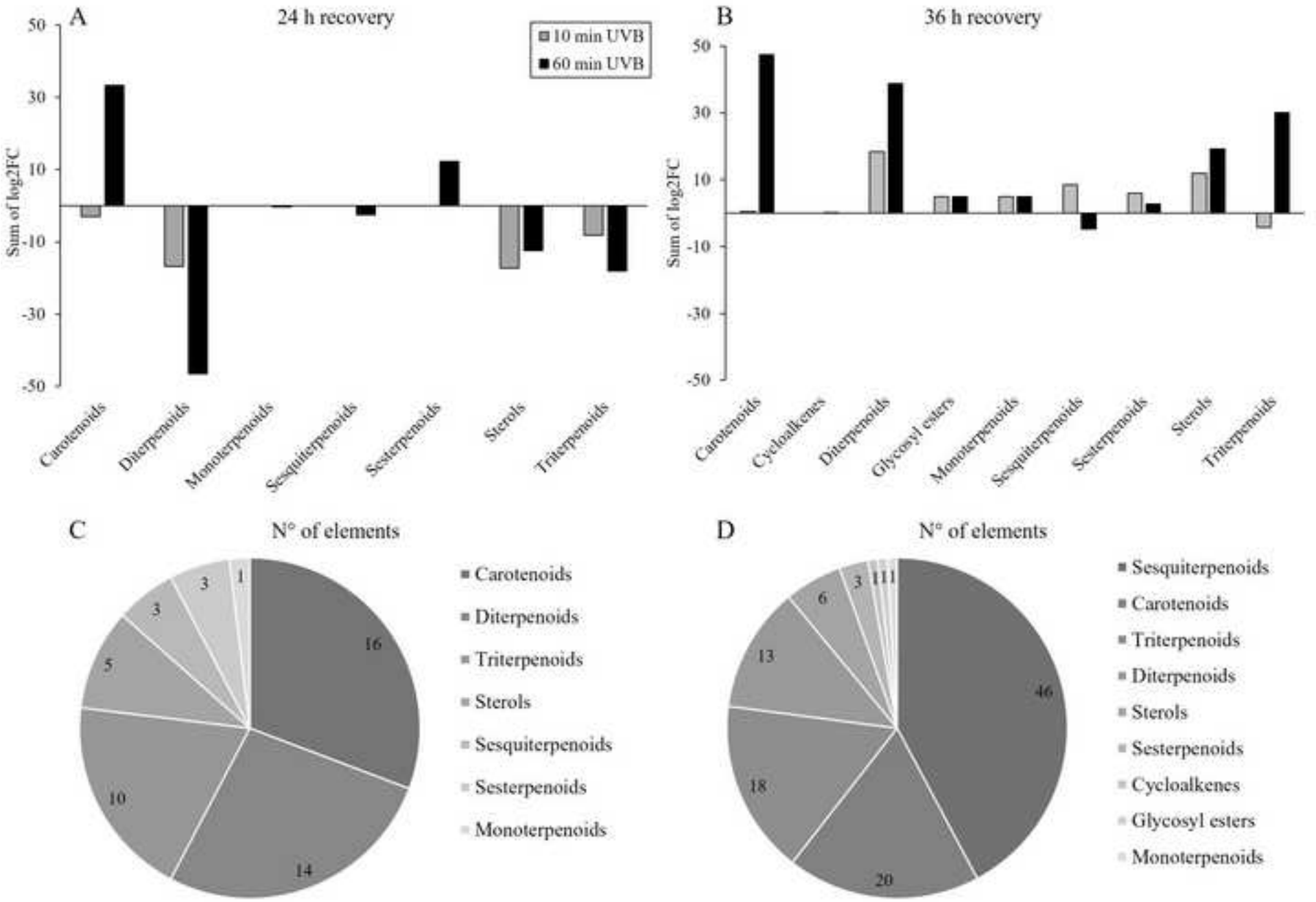

Figure 6

Click here to download high resolution image

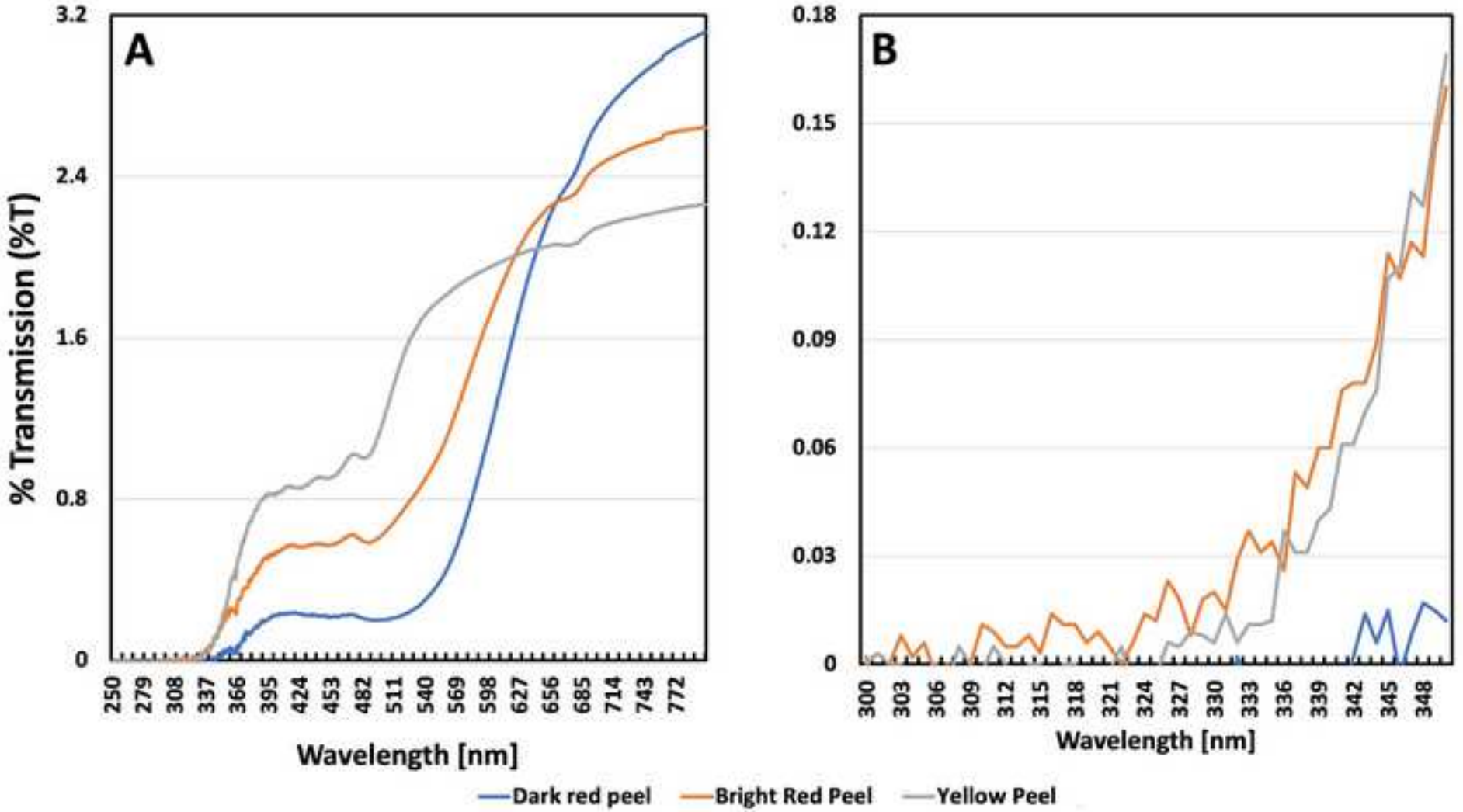

Supplementary Figure S1

Click here to download high resolution image

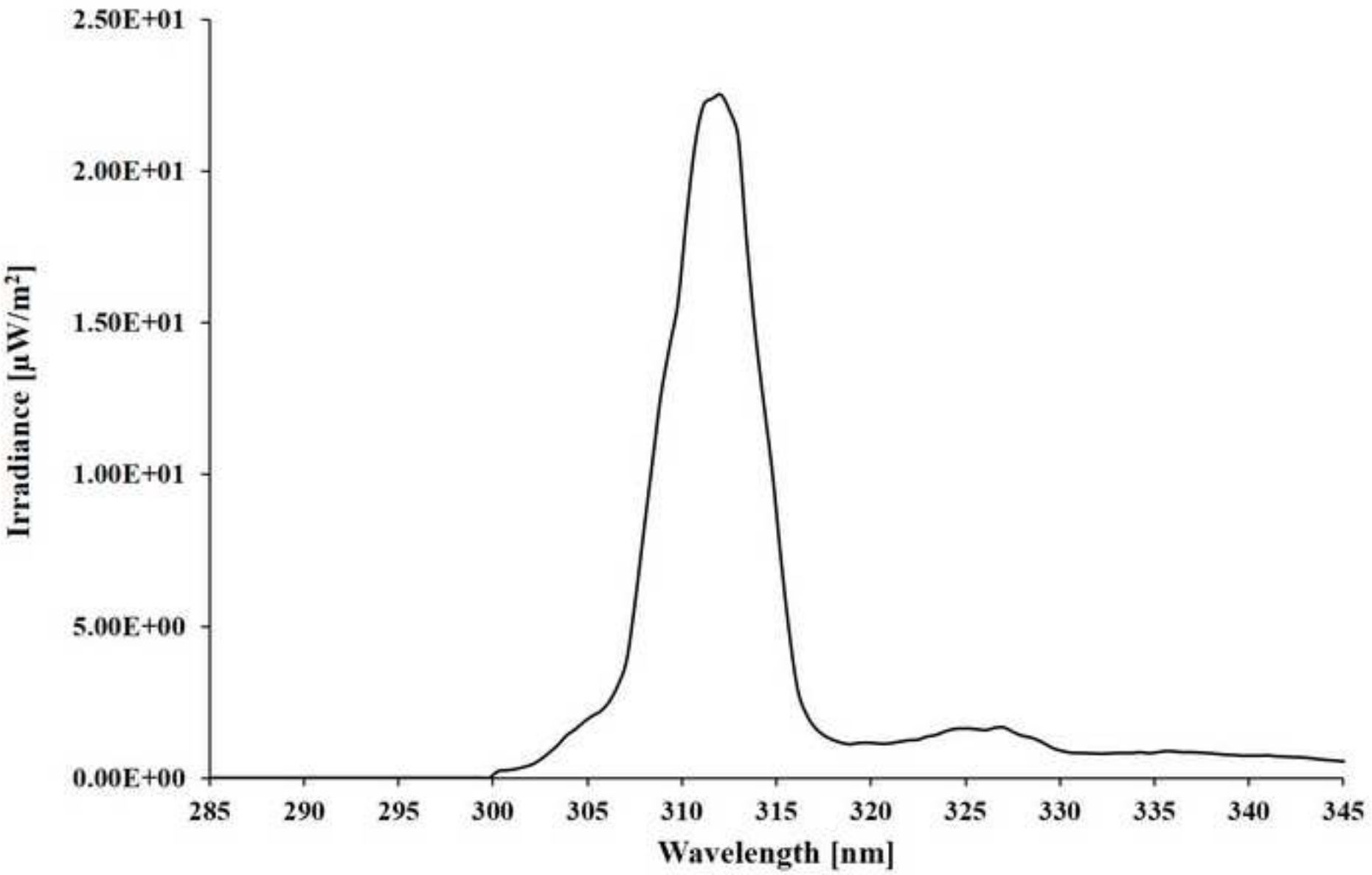

Supplementary Figure S2
Click here to download high resolution image

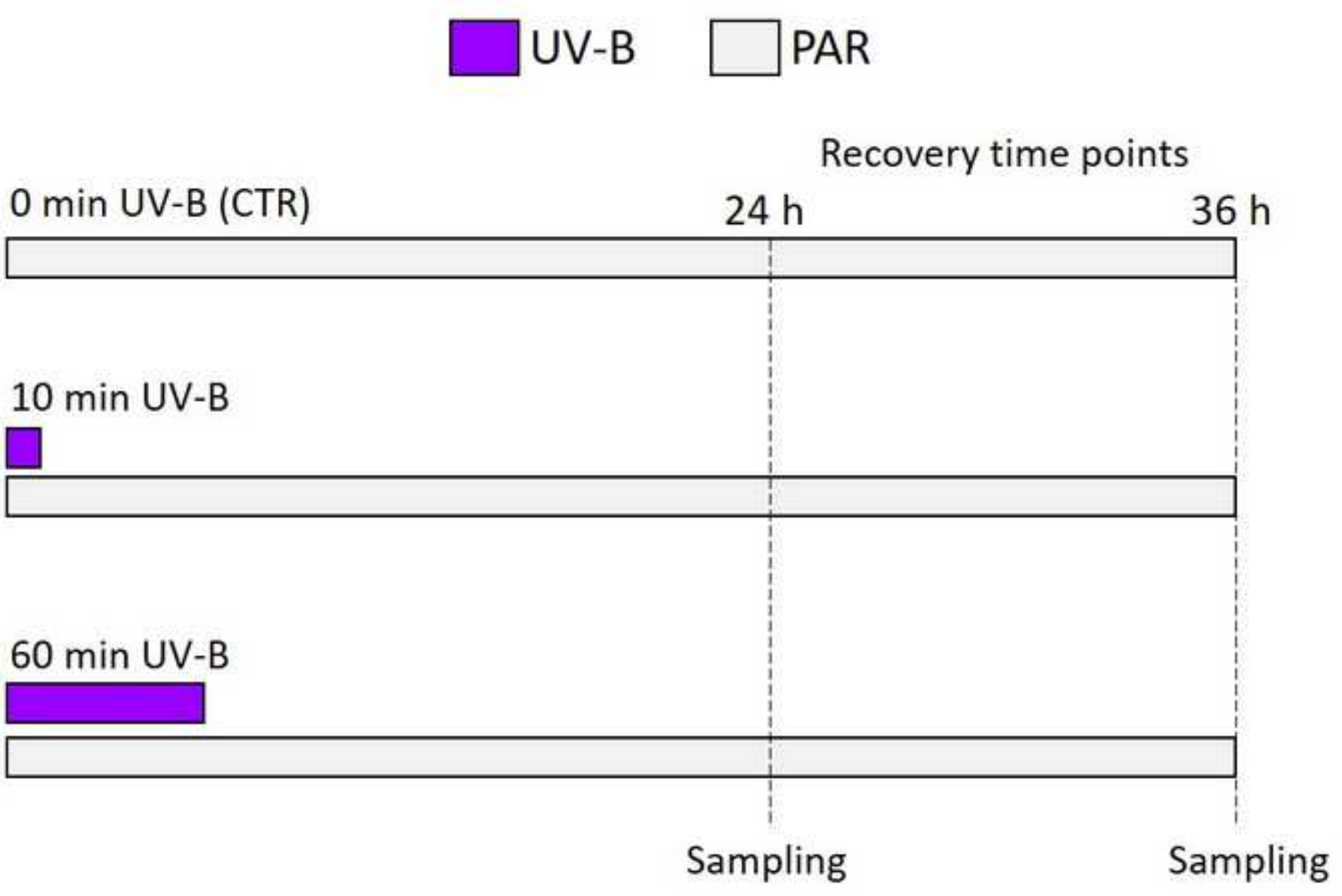

Supplementary Table S1

Click here to download Supplementary Material: Table S1. Phenol-Explorer dataset.xlsx

Compound	Phenolic class
Pelargonidin 3,5-O-diglucoside	Flavonoids
Pelargonidin 3-O-rutinoside	Flavonoids
Delphinidin 3-O-glucoside	Flavonoids
Delphinidin 3,5-O-diglucoside	Flavonoids
Peonidin	Flavonoids
Peonidin 3-O-galactoside	Flavonoids
Cyanidin 3-O-glucoside	Flavonoids
Pinotin A	Flavonoids
Petunidin 3-O-(6''-acetyl-galactoside)	Flavonoids
Delphinidin 3-O-rutinoside	Flavonoids
Malvidin 3,5-O-diglucoside	Flavonoids
Cyanidin 3,5-O-diglucoside	Flavonoids
Pelargonidin 3-O-galactoside	Flavonoids
Cyanidin 3-O-xyloside	Flavonoids
Pelargonidin 3-O-(6''-malonyl-glucoside)	Flavonoids
Cyanidin 3-O-(6''-acetyl-glucoside)	Flavonoids
Petunidin 3-O-(6''-acetyl-glucoside)	Flavonoids
Pelargonidin 3-O-glucosyl-rutinoside	Flavonoids
Petunidin 3-O-(6''-p-coumaroyl-glucoside)	Flavonoids
Delphinidin 3-O-sambubioside	Flavonoids
Pelargonidin	Flavonoids
Pelargonidin 3-O-glucoside	Flavonoids
Delphinidin 3-O-glucosyl-glucoside	Flavonoids
Cyanidin 3-O-(6''-p-coumaroyl-glucoside)	Flavonoids
Delphinidin 3-O-(6''-acetyl-glucoside)	Flavonoids
Malvidin 3-O-(6''-caffeoyl-glucoside)	Flavonoids
Pelargonidin 3-O-arabinoside	Flavonoids
Delphinidin 3-O-(6''-p-coumaroyl-glucoside)	Flavonoids
Cyanidin 3-O-glucosyl-rutinoside	Flavonoids
Petunidin 3-O-glucoside	Flavonoids
Delphinidin 3-O-(6''-acetyl-galactoside)	Flavonoids
Cyanidin 3-O-sophoroside	Flavonoids
Malvidin 3-O-(6''-p-coumaroyl-glucoside)	Flavonoids
Malvidin 3-O-arabinoside	Flavonoids
Peonidin 3-O-glucoside	Flavonoids
Malvidin 3-O-(6''-acetyl-glucoside)	Flavonoids
Petunidin 3-O-rutinoside	Flavonoids
Pigment A	Flavonoids
Pelargonidin 3-O-sophoroside	Flavonoids
Cyanidin 3-O-xylosyl-rutinoside	Flavonoids
Petunidin 3-O-rhamnoside	Flavonoids
Petunidin 3-O-arabinoside	Flavonoids
Cyanidin 3-O-(6''-caffeoyl-glucoside)	Flavonoids
Cyanidin 3-O-arabinoside	Flavonoids
Delphinidin 3-O-galactoside	Flavonoids
Cyanidin 3-O-sambubioside 5-O-glucoside	Flavonoids

Supplementary Table S2

Click here to download Supplementary Material: Table S2. PlantCyc dataset.xls

Ontology - parents of class	Compound	[10'_24h]	[10'_36h]	[60'_24h]
glucocorticoid	cortisol	0.087568	0.030614	-8.51755
α-selinene	7-epi-α-selinene	-0.95898	0.58852	-1.72212
α-terpineol	(-)-(4S)-α-terpineol	7.789772	3.921909	3.99678
β bitter acid	colupulone	0.38232	-0.37627	1.253443
β bitter acid	adlupulone	-9.86675	-10.0202	-14.9053
β bitter acid	lupulone	-0.5008	-1.16112	-0.93895
β-D glucoside	salicin	-0.07582	0.405351	3.296211
β-D glucoside // "methyl-D-gl	methyl β-D-glucoside	0.220199	0.399521	-4.93157
β-D glucoside // "nitrile"	taxiphyllin	13.71616	4.314822	4.358428
β-D glucoside // "pyranoside'	p-nitrophenyl-β-D-glucopyra	-0.17102	0.109239	-0.53645
β-D-galactoside	methyl-β-D-galactoside	0.220199	0.399521	-4.93157
β-phellandrene	(-)-β-phellandrene	-6.72488	-10.7448	-10.5234
Δ¹⁴steroid	4α-methyl-5α-ergosta-8,14,	-0.29196	4.40001	4.21339
Δ¹⁴steroid // "3	4,4-dimethyl-cholesta-8,12,24-trienol	-0.29196	4.40001	4.21339
Δ¹⁴steroid // "3	4α-methyl-5α-cholesta-8,14	-0.2408	-4.92787	-4.7502
Δ5,7-sterol	5-dehydroavenasterol	-0.29196	4.40001	4.21339
Δ5,7-sterol	ergosta-5,7,24(28)-trien-3β-ol	4.584589	4.831015	9.601992
Δ5,7-sterol	poriferst-5,7-dienol	4.502921	-0.01356	8.977541
Δ5,7-sterol	ergosta-5,7-dienol	9.484967	13.9141	4.871165
Δ5,7-sterol // "3β-hydr	7-dehydrodesmosterol	0.134962	-0.35598	-0.15713
Δ5,7-sterol // "3β-hydr	7-dehydrocholesterol	4.206201	8.433466	-0.02278
Δ7-sterol	poriferst-7-enol	-5.04014	0.193042	-0.17687
Δ7-sterol	ergost-7-enol	0.190497	0.458164	0.158795
Δ7-sterol	episterol	9.484967	13.9141	4.871165
Δ7-sterol // "3β-hydro	5α-cholesta-7,24-dien-3β-ol	4.206201	8.433466	-0.02278
Δ7-sterol // "3β-hydro	lathosterol	-5.28115	-12.407	-4.61336
Δ7-sterol // "triterpenoid"	avenasterol	4.502921	-0.01356	8.977541
δ-lactone	O-sinapoylglucarolactone	0.109092	2.7801	1.922181
δ-lactone	D-glucaro-1,5-lactone	-0.01426	0.001435	0.029988
δ-lactone	triacetate lactone	-10.7719	-10.5385	-2.7586
δ-selinene	(+)-δ-selinene	-0.95898	0.58852	-1.72212
γ-lactone	2-keto-4-hydroxybutyrolactone	-0.59478	-4.00016	-0.10245
γ-lactone	L-galactono-1,4-lactone	7.310908	3.516268	7.341246
γ-lactone	D-galactaro-1,4-lactone	-0.01426	0.001435	0.029988
ω-3 fatty acid // "long-chai	docosahexaenoate	0.138108	0.673657	3.054953
ω-3 fatty acid // "long-chai	α-linolenate	0.560693	0.658899	0.010957
ω-3 fatty acid // "long-chai	icosatetraenoate	4.523052	9.128118	9.217981
ω-3 fatty acid // "long-chai	stearidonate	-0.36576	-9.85592	-3.53799
ω-3 fatty acid // "long-chai	icosapentaenoate	-0.28953	-0.00646	1.502441
ω-6 fatty acid // "an icosatr	di-homo-γ-linolenate	-6.01667	-12.0653	-6.05132
ω-6 fatty acid // "long-chai	linoleate	-0.04473	0.115232	0.212172
ω-6 fatty acid // "long-chai	arachidonate	4.523052	9.128118	9.217981
(22R,23R)-28-homobrassinc	(22R,23R)-28-homobrassinolide 2	-0.16268	0.242567	-4.41709
(22R,23R)-28-homocastaste	(22R,23R)-28-homocastasterone 2	-0.09553	-0.1988	0.076115
(E)-nerolidol	(3S,6E)-nerolidol	-8.30214	-16.9903	-0.26877
(E)-nerolidol	(3R,6E)-nerolidol	-8.30214	-16.9903	-0.26877

Supplementary Table S3

Click here to download Supplementary Material: Table S3. Volcano analysis.xls

Compound CPD
CPD-8198
CPD-12398
CPD-4608
CPD-3141
CPD-15373
CPD0-2099
CPDQT-422
CPD-8290
CPD-4750
CPD-10894
CPD-15449
CPD-13255
CPD-7246
CPD-14842
CPD-9462
ALLYSINE
CPD-10678
CPD0-1028
GERANYLGERANYL-PP
ALPHA-METHYL-5-ALPHA-ERGOSTA
CPD-9502
CPD-12510
CPD-13086
44-DIMETHYL-CHOLESTA-812-24-TRIENOL
CPD-4126
CPD-12868
CAFFEOYLSHIKIMATE
PHENYLACETALDEHYDE
CPD-12815
CPD-11595
CPD-14912
CPD-19480
CPDIO2-5
CPD-14899
CPD-7192
CPDQT-16
44-DIMETHYL-CHOLESTA-814-24-TRIENOL
CPD-15977
910-EPOXY-18-HYDROXYSTEARATE
CPD-9896
D-ERYTHRO-IMIDAZOLE-GLYCEROL-P
CPD-11394
CPD-15177
ENT-COPALYL-DIPHOSPHATE
CPD-13544
CPD-12920